IEEE Access
Multidisciplinary | Rapid Review | Open Access Journal

Received 26 February 2025, accepted 11 March 2025, date of publication 14 March 2025, date of current version 7 April 2025.

*Digital Object Identifier 10.1109/ACCESS.2025.3551398*

RESEARCH ARTICLE

# Multi-User Sparse Vector Coding for eXtreme Ultra-Reliable Low-Latency Communication in Beyond 5G

**SUNDARESAN SABAPATHY[1], (Member, IEEE), SURENDAR MARUTHU[2], (Member, IEEE), AND DUSHANTHA NALIN K. JAYAKODY[3,4,5], (Senior Member, IEEE)**

[1]School of Artificial Intelligence, Amrita Vishwa Vidyapeetham, Coimbatore, Tamil Nadu 641112, India
[2]Department of Electronics and Communication Engineering, National Institute of Technology Puducherry, Karaikal 609609, India
[3]COPELABS, Lusofona University, Lisbon 1749–024, Portugal
[4]Center of Technology and Systems (UNINOVA-CTS) and Associated Lab of Intelligent Systems (LASI), Caparica 2829-516, Portugal
[5]CIET/DEEE, Faculty of Engineering, Sri Lanka Institute of Information Technology, Malabe 10115, Sri Lanka

Corresponding authors: Dushantha Nalin K. Jayakody (dushantha.jayakody@ulusofona.p) and Sundaresan Sabapathy (S_Sundaresan@cb.amrita.edu)

This work was supported in part by the Sri Lanka Institute of Information Technology through the grant PVC(R&I)/RG/2024/12, by the European Commission via Marie Skłodowska-Curie Actions (MSCA) as part of the project REMARKABLE (No. 101086387), by the COFAC - Cooperativa de Formação e Animação Cultural, C.R.L. (University of Lusófona University), via the project PortuLight (COFAC/ILIND/COPELABS/2/2023), by the national funds through FCT - Fundação para a Ciência e a Tecnologia - as part of the projects URLLC-UAV (2023.08191.CEECIND), Center of Technology and Systems (UNINOVA-CTS) (UIDB/00066/2020) and COPELABS (no. UIDB/04111/2020), and by the Scheme for Promotion of Academic & Research Collaboration (SPARC), Government of India, via grant no. SPARC/2024-2025/NXTG/P3524.

**ABSTRACT** Short A short packet transmission scheme, such as Sparse Vector Coding (SVC), is a primary candidate for achieving ultra-low latency and high-reliability communication (URLLC). This paper proposes a spectral-efficient multi-user SVC (MU-SVC) scheme for achieving next-generation URLLC or eXtreme URLLC (xURLLC) in beyond 5G (B5G) communications. The key idea is to transmit multiple user information within a single sparse vector where the users are segregated into far users (FU) and near users (NU) depending on the distance from the base station. The classification into FU and NU paves way to optimize resource allocation, user fairness, manage interference, ensure reliable communication and quality of service requirements. Firstly, the FU binary data is converted into a sparse vector and secondly, the NU data is modulated and embedded into the non-zero positions of the sparse vector to form an MU-SVC. On transmission, the FU data is obtained through sparse demapping, while the NU adopts symbol detection techniques like the maximum likelihood detector. A new performance metric, called position error rate (PoER), is introduced to study the performance of the FU since it is based on the correct identification of the non-zero positions. Theoretical analyses of PoER and symbol error rate (SER) were carried out for FU and NU, respectively and the results are also validated through Monte-Carlo simulations. Further, the bit error rate, complexity, spectral and latency analyses are performed for MU-SVC and compared with the SVC and enhanced SVC schemes. The simulation results demonstrate an improved spectral efficiency and low latency with high reliability for the proposed MU-SVC scheme, thus, achieving xURLLC with reduced complexity in the multi-user scenario for B5G.

**INDEX TERMS** Multi-user, position error rate, sparse vector coding, superimposed transmission, symbol error rate, URLLC.

## I. INTRODUCTION

ULTRA-reliable and low-latency communication (URLLC) is gathering keen attention in fifth generation (5G) wireless systems due to an increase in time-critical and round-the-clock accessible applications. URLLC is designed to deliver communication services with extremely high levels of reliability. This is crucial for applications where even a small amount of packet loss or communication failure could have serious consequences, such as in industrial

The associate editor coordinating the review of this manuscript and approving it for publication was Mostafa Zaman Chowdhury.

automation, remote surgery, autonomous vehicles, and public safety scenarios [1], [2], [3]. URLLC plays a crucial role in the context of intelligent transportation systems (ITS), autonomous driving where vehicles, infrastructure, and other elements need to communicate quickly and reliably to ensure safety and efficiency [4], [5]. Moreover, most of the applications require only tiny information to transmit such as moving forward/backward, turning left/right, on/off, etc., (control signals) and hence demand efficient transmission control. Short packet transmission is a key enabler of URLLC which addresses the need for both low latency and reliable data transmission in applications that require real-time interactions and critical reliability, making it a fundamental aspect of modern wireless communication systems. The benchmark for URLLC is 99.99% reliability with less than 1ms latency and one in a million block error rate (BLER) [6], [7], [8], [9], [10], [11]. In par with this, sparse vector coding (SVC) is proposed in [12] for transmission of short packets to achieve URLLC. The idea is to explore the sparse nature of the information and get rid of conventional channel coding schemes which require lengthy codes with complex nature [12], [13], [14], [15].

In SVC, the information is sparsely mapped with the minimum number of non-zero elements and pseudo-randomly spread through a code book (dictionary matrix) at the transmitter. This information is then transmitted over the channel and at the receiver, the signal is considered to be undetermined. To address this, compressed sensing (CS) based sparse recovery algorithms (SRA) [16], [17] are aided for successful decoding of the information. A probability of success analysis is carried out and shows that SVC supports URLLC. Likewise in [12], [13], [14], [15], [18], and [19], BLER analysis is performed for SVC with various parameters which depend on less pilot overload and pilot-less transmission. Recently, an enhanced SVC (ESVC) scheme was proposed for URLLC in which the information is encoded as symbols in addition to position for enhancing the reliability [20]. At the receiver, the support is identified through SRA, and symbols are detected by conventional techniques. From the performance analysis, it is depicted that SVC is less efficient than ESVC. In addition, SVC for massive multiple-input multiple-output (MIMO) is proposed in [21] which transmits information through multi-antenna system. At the receiver, successive cancellation is carried out to decode the intended user information.

Moreover, SVC is exploited with multi-carrier non-orthogonal multiple access (MC-NOMA) for in-home health networks [22] in which the inter carrier interference (ICI) suppression is achieved due to sparse nature of the information transmitted. To further enhance the performance of SVC, the constellation group based rotation technique is adopted in [23] which maps the information bits to sparse vectors ensuring that the minimum Euclidean distance between the constellation is large. Also in [24] sparse superimposed transmission (ST) is exploited for SVC in which a certain amount of information is sparsely mapped and the remaining part of the information is mapped to non-zero positions through constellation rotation. Simulation results show that the SVC-ST scheme performance is superior in terms of BLER.

Furthermore, to enhance the reliability, ESVC with the limited pilot overhead is explored in which the sparse vector is scaled by the fading channel and decoding does not require any channel state information [25]. Also, the sparse vector is composited with maximal ratio transmission over the channel for enhancing the reliability of the system in [26]. Additionally, to enhance the performance of SVC, a superimposed transmission technique is adopted in [27]. The encoding is done by sparse mapping a certain part of user information into non-zero sparse vector and remaining part is quadrature amplitude modulated through constellation rotation. Besides, SVC is also aided for integrated sensing and communication applications [28] for enhancing the reliability and attenuating the side lobes of radar signals. The information is sparse mapped and the control for reducing the side lobes of the radar signal are embedded into the spreading code, thus ensuring reliability with lower lobes for radar sensing. An optimized code book or resource element is utilized in [29] for spreading the sparse vector to enhance the reliability, reduce complexity and hardware realization in URLLC applications.

Also, outage analysis of SVC is carried out for MC-NOMA in [30] and shown that SVC aids for suppressing the ICI in multi-carrier communication and contributes for URLLC. Yet importantly, SVC is exploited for high mobility scenario with Doppler effect in [31] which accounts the time varying channel parameters. The data and the pilots for estimating the time varying channel is sparse mapped at the transmitter which is then pseudo randomly spread over a random spreading code. At the receiver, the decoding of data by canceling out the pilots is performed through iterative interference cancellation and the channel is estimated by iterative data-aided process. Nevertheless, sixth-generation (6G) communication aims to address next-generation use cases while building upon and enhancing those introduced by 5G. This includes the need for achieving extreme URLLC capabilities surpassing those in 5G. In aim of this, SVC is exploited with rate splitting approach in [32] and shown that along with xURLLC, SVC supports enhanced data rate in B5G applications.

xURLLC in the context of ITS, industrial 4.0 and 5.0, etc., can enable a variety of applications and services. To mention a few, vehicle-to-everything (V2X) communication, traffic management, infrastructure monitoring, robotic surgery, truck platooning, etc. In applications such as autonomous vehicles and truck platooning, the amount of information transferred is petite but the number of devices/users connected is large and demands for spectrum efficient communication [33], [34], [35], [36]. Thus, xURLLC along with spectral efficiency to support massive connectivity is

**TABLE 1. List of symbols.**

| Abbreviation | Definition |
|---|---|
| 3GPP | Third Generation Partnership Project |
| B5G | Beyond Fifth Generation |
| 6G | Sixth Generation |
| BER | Bit Error Rate |
| BLER | Block Error Rate |
| BS | Base Station |
| CS | Compressed Sensing |
| CSI | Channel State Information |
| ESVC | Enhanced Sparse Vector Coding |
| FU | Far User |
| ICI | Inter Carrier Interference |
| ITS | Intelligent Transportation System |
| LUT | Look Up Table |
| MC-NOMA | Multicarrier Non Orthogonal Multiple Access |
| MIMO | Multiple Input Multiple Output |
| MU | Multi User |
| MU-SVC | Multi-User Sparse Vector Coding |
| NU | Near User |
| OMP | Orthogonal Matching Pursuit |
| PER | Packet Error Rate |
| PoER | Position Error Rate |
| QPSK | Quadrature Phase Shift Keying |
| SER | Symbol Error Rate |
| SNR | Signal-to-Noise Ratio |
| SRA | Sparse Recovery Algorithm |
| ST | Superimposed Transmission |
| SVC | Sparse Vector Coding |
| URLLC | Ultra-Reliable Low-Latency communication |
| xURLLC | eXtreme URLLC |
| V2X | Vehicle-to-Everything |

of keen interest in B5G communications. The main aim of this paper is to simultaneously serve multiple users at various distances from the base station (BS) with a single sparse vector through a single transmission, thereby enhancing spectral occupancy and supporting xURLLC applications.

In this paper, a novel MU short packet transmission scheme is enabled through a sparse vector for xURLLC. The users are classified as far users (FU) and near users (NU) based on their distance from the base station. The BS does not require the exact physical distance of each user; instead, it classifies users as FU or NU based on their known Channel State Information (CSI). Since CSI inherently reflects the effects of path loss, shadowing, and fading, the BS can estimate relative distances or categorize users by comparing their channel gains. Users experiencing higher path loss and weaker channel gains are classified as FUs, while those with lower path loss and stronger channel gains are classified as NUs. This classification allows the BS to optimize power allocation, ensuring that far users receive higher transmission power to maintain fairness and enhance overall spectral efficiency. This aids in serving multiple users, simultaneously on the same time-frequency resource (ensuring effective utilization of resources), through superimposed transmission. In turn, this will result in optimized resource allocation, enhance user fairness, manage interference, ensure reliable communication, reduce latency (at the system level), and meet quality-of-services requirements. Initially, information of the FU is encoded into a sparse vector and the NU information is converted to symbols. Now, the symbols are embedded into the position of non-zero elements in the FU sparse vector. This superimposed signal is pseudo-randomly spread through a code book and transmitted over the channel. At the receiver's end, the support identification is performed through SRA along with sparse demapping and symbol detection in FU and NU, respectively. The proposed MU-SVC supports the transmission of multiple users' data in a single sparse vector, rather than utilizing individual sparse vectors as in traditional SVC. The key advantage of the proposed MU-SVC scheme over ESVC is that FU and NU can obtain their information by decoding only the non-zero positions and symbols, respectively. Also, optimal power allocation is not required for NU and FU in MU-SVC. Moreover, in this paper position error rate (PoER) and symbol error rate (SER) analyses are performed which shows the proposed scheme is much more reliable with low latency. Furthermore, spectral efficiency, user fairness along with MU connectivity are also achieved for xURLLC. For ease of reference, Table 1 summarizes the list of symbols. The fore-fold contributions of this paper are summarized here:

- A novel spectral efficient MU-SVC transmission scheme for xURLLC has been proposed for MU environments.
- It is shown that MU-SVC serves more than one user simultaneously, without any compromise in latency and reliability standards of ESVC.
- A new performance metric viz., PoER has been computed to analyse the reliability of the proposed system and also its significance is discussed.
- Numerical analysis in terms of PoER and SER has been carried out for the proposed MU-SVC scheme and validated through Monte-Carlo simulations.
- Furthermore, bit error rate (BER), complexity, spectral occupancy and transmission latency analyses are performed for MU-SVC and compared with existing SVC techniques.

The rest of this paper is organized as follows. Section II describes the proposed system model with encoding and decoding procedures. The significance of PoER, numerical performance analysis in terms of PoER, SER, BER, computational complexity and spectral occupancy are put forth in Section III. Section IV presents the simulation results of the MU-SVC scheme with various key parameters and a comparison with the existing schemes followed by conclusion in Section V.

## II. MULTI-USER SPARSE VECTOR CODING

Consider a downlink scenario where multiple users need to be served by the BS for short packet transmission in URLLC. With the objective of meeting the xURLLC target defined by third generation partnership project (3GPP) [11] and striving to attain spectral efficiency while ensuring fairness among users, an MU-SVC scheme is proposed which exploits SVC and superimposed techniques. Multiple users at the receiver end are grouped as FU and NU based on the

**Algorithm 1** Pseudo-Code for the MU-SVC Scheme

**Input:** Length of the sparse vector ($N$), Number of users ($U$), FU Information ($W$), NU symbols ($x_U$), Sparsity ($K$)
**Output:** MU-Sparse vector ($\mathbf{s}$)
*Initialisation*: $p = 0$
**for** $a = 2$ to $N$ **do**
  **for** $b = 1$ to $a - 1$ **do**
    **if** $p = (W)$ **then**
      $\tilde{\mathbf{s}} = (2^{(a-1)} + 2^{(b-1)})$
    **end if**
    $p = p + 1$
  **end for**
**end for**
$\mathbf{s} = indexmod[\tilde{\mathbf{s}}(x_U)]$
**return** $\mathbf{s}$

distance from the BS. Initially, at the BS, FU information is mapped to sparse vector $\tilde{\mathbf{s}}$ with sparsity $K$ and sparse vector length $N$. Now, the NU information is transformed into symbols through modulation techniques and the symbols are embedded into the position of non-zero elements of the FU sparse vector which results in an embedded sparse vector $\mathbf{s}$. The pseudo-code for generation of MU-SVC from FU and NU data is described in Algorithm 1. The number of bits that can be encoded is obtained as $b = \left\lfloor log_2\binom{N}{K} \right\rfloor$. Subsequently, each sparse vector is spread into $m$ physical resource through pseudo-random spreading. Let the non-zero elements of FU be at the $p^{th}$ and $q^{th}$ positions in which the NU symbols are embedded and its vector is represented mathematically as,

$$\mathbf{x} = \mathbf{S}_p^{NU}\mathbf{C_p} + \mathbf{S}_q^{NU}\mathbf{C_q} \tag{1}$$

where, $\mathbf{S}_p^{NU}$ and $\mathbf{S}_q^{NU}$ are the NU symbols at the $p^{th}$ and $q^{th}$ positions. The code book matrix is designed precisely by random Bernoulli distribution with dimension $\mathbf{C} = (m \times N)$ in which $m < N$ such that the sensing matrix ($\mathbf{x} = \mathbf{Cs}$) holds enough information for recovering the sparse vector, where $m$ is the number of resource elements. The random code book matrix can be realized as in (2) with equal probabilities of 1 and $-1$.

$$\mathbf{C} = \frac{1}{\xi}\begin{bmatrix} 1 & -1 & 1 & \cdots & \cdots & \cdots & 1 \\ -1 & -1 & 1 & \ddots & & & \vdots \\ 1 & 1 & -1 & 1 & \ddots & & \vdots \\ \vdots & \ddots & \ddots & \ddots & \ddots & \ddots & \vdots \\ \vdots & \ddots & \ddots & \ddots & \ddots & \ddots & \vdots \\ \vdots & \cdots & \cdots & -1 & 1 & -1 & -1 \end{bmatrix}_{(m\times N)} \tag{2}$$

where $\xi$ is the normalization factor based on the modulation technique aided. Conventionally, for symbol encoding $M$-ary quadrature phase shift keying (QPSK) modulation is utilized and its normalization is calculated as $\xi = \sqrt{\frac{2(M+1)}{3}}$ in which $M$ is the order of modulation. After spreading, the sparse signal is transmitted over the Rayleigh channel with independent and identically distributed noise ($\upsilon$) which is expressed as, $\mathbf{y} = \mathbf{Hx} + \boldsymbol{\nu}$, where $\mathbf{H}$ is a diagonal matrix representing the channel coefficients, and can be visualized as,

$$\mathbf{y} = \begin{bmatrix} \mathbf{h}_{11} & \cdots & \mathbf{h}_{1m} \\ \vdots & \ddots & \vdots \\ \mathbf{h}_{m1} & \cdots & \mathbf{h}_{mm} \end{bmatrix} \begin{bmatrix} \mathbf{c}_1 & \cdots & \mathbf{c}_N \end{bmatrix} \begin{bmatrix} \mathbf{s}_1 \\ \vdots \\ \mathbf{s}_N \end{bmatrix} + \begin{bmatrix} \mathbf{v}_1 \\ \vdots \\ \mathbf{v}_m \end{bmatrix} \tag{3}$$

Thus, the received signal-to-noise ratio (SNR) at any specific user ($U$) can be expressed as,

$$\text{SINR}_U = \frac{P_U \left| \mathbf{h}_{p,U}\mathbf{S}_p^{NU} + \mathbf{h}_{q,U}\mathbf{S}_q^{NU} \right|^2}{\sum\limits_{j\neq U} P_j \left| \mathbf{h}_{p,j}\mathbf{S}_p^{NU} + \mathbf{h}_{q,j}\mathbf{S}_q^{NU} \right|^2 + \boldsymbol{\sigma}^2} \tag{4}$$

where $P_U$ is the transmit power allocated to user $U$, $\mathbf{h}_{p,U}$ and $\mathbf{h}_{q,U}$ are the Rayleigh fading coefficients for user $U$ at positions $p$ and $q$, with probability density function (PDF) given by $f_\gamma(\gamma) = \frac{1}{\bar{\gamma}} e^{-\gamma/\bar{\gamma}}, \quad \gamma \geq 0$ in which $\bar{\gamma}$ is the average SNR, $P_j$ and $\mathbf{h}_{p,j}$, $\mathbf{h}_{q,j}$ represent the power and channel coefficients for interfering users $j \neq U$, respectively, and $\boldsymbol{\sigma}^2$ is the noise power. Since FU data is sparsely mapped and NU symbols are embedded in FU positions, interference terms differ and the SNR for FU is mathematically written as,

$$\text{SINR}_{\text{FU}} = \frac{P_{\text{FU}} \sum\limits_{i\in\boldsymbol{\mathcal{S}}_{\text{FU}}} |\mathbf{h}_i\mathbf{S}_i^{\text{FU}}|^2}{\sum\limits_{j\neq\text{FU}} P_j \sum\limits_{k\in\boldsymbol{\mathcal{S}}_j} |\mathbf{h}_k\mathbf{S}_k^j|^2 + \boldsymbol{\sigma}^2} \tag{5}$$

where $\mathcal{S}_{\text{FU}}$ represents the set of active sparse positions assigned to FU. Similarly, the SNR for the NU can be written as,

$$\text{SINR}_{\text{NU}} = \frac{P_{\text{NU}} \sum\limits_{p,q} |\mathbf{h}_p\mathbf{S}_p^{\text{NU}} + \mathbf{h}_q\mathbf{S}_q^{\text{NU}}|^2}{\sum\limits_{j\neq\text{NU}} P_j \sum\limits_{k\in\boldsymbol{\mathcal{S}}_j} |\mathbf{h}_k\mathbf{S}_k^j|^2 + \boldsymbol{\sigma}^2} \tag{6}$$

On the other side, the sparse signal seems to be an undetermined system in nature and requires CS techniques [37], [38] for the detection of non-zero position which turns out to be a determined system.

Fig. 1 sketches the encoding block diagram of the proposed MU-SVC scheme at the BS whereas, Fig. 2 (a) and Fig. 2(b) shows the decoding process of MU-SVC at the FU and NU respectively. At the FU, support identification is carried out through greedy algorithms such as orthogonal matching pursuit (OMP) from which the non-zero positions are identified. To aid SRA, it is taken care that $m \leq \mathcal{O}(K\log N)$ for support identification [4]. In OMP, the sparse mapped information is projected onto the sensing matrix and correlation between each column in $\boldsymbol{\phi}$ is obtained. Since, $\mathbf{S}$ contains only $K$ non-zero elements, the received signal $\mathbf{y}$ can be represented as a linear combination of $K$ selected columns from the matrix $\Phi = \mathbf{HC}$, with an additional noise component which can be expressed as, $\mathbf{y} = \Phi\mathbf{s} + \boldsymbol{\nu}$. The

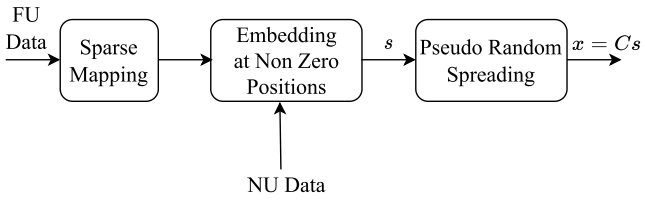


**FIGURE 1.** MU-SVC encoding scheme at the BS.

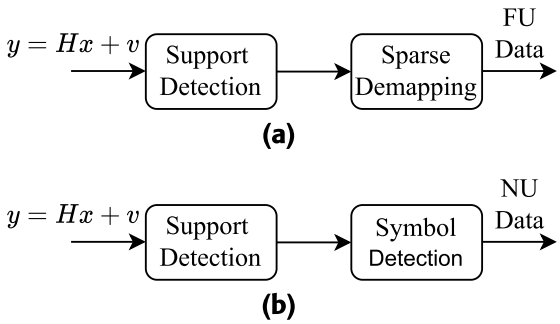


**FIGURE 2.** MU-SVC decoding scheme at (a) FU (b) NU.

maximum correlation column is considered for each non-zero element and the residual factor is updated in each iteration. The index of the support estimated at $p$-th iteration is given by,

$$\omega_p = \arg \max_{1 \le n \le N} \left| \left\langle \boldsymbol{\phi}_n, r^{p-1} \right\rangle \right|^2. \tag{7}$$

where $r$ is the residual factor. Once the support ($\hat{\Omega}$) is identified, sparse demapping is performed to decode the FU information through look up table (LUT) approach. Likewise, support identification is performed at the NU and symbol detection is computed to decode the information. The main contribution of the MU-SVC is that despite adopting the superimposed principle, each user can decode their information simultaneously. Moreover, power can be concentrated in non-zero positions rather than optimal power allocation for the FU and NU. The allegorical representation of MU-SVC is sketched in Fig. 3 for ease of understanding. Table 2 displays the mapping of FU and NU data into superimposed sparse vectors for a specific scenario and this can be extended to any number of users and sparse vectors without loss of generality. Fig. 4 portrays the downlink scenario of the proposed MU-SVC scheme for xURLLC applications. In MU-SVC scheme, the encoding and decoding strategies for FU and NU are distinct. Specifically, FU information undergoes sparse mapping, resulting in a sparse vector with non-zero entries corresponding to FU data. NU data, on the other hand, is symbol-modulated and embedded into the non-zero positions of the sparse-mapped FU data. The resultant sparse vector is then pseudo-randomly spread. During decoding, the superimposed signal received by both FU and NU is processed differently. For FU, the data is retrieved using support detection combined with sparse de-mapping, bypassing the need for symbol demodulation.

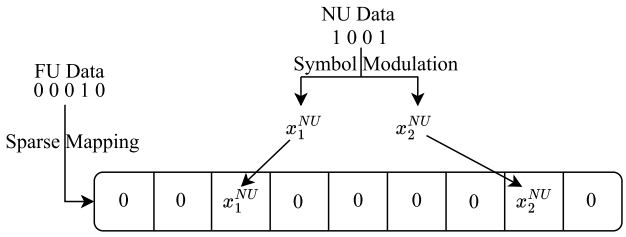


**FIGURE 3.** Allegorical representation of MU-SVC.

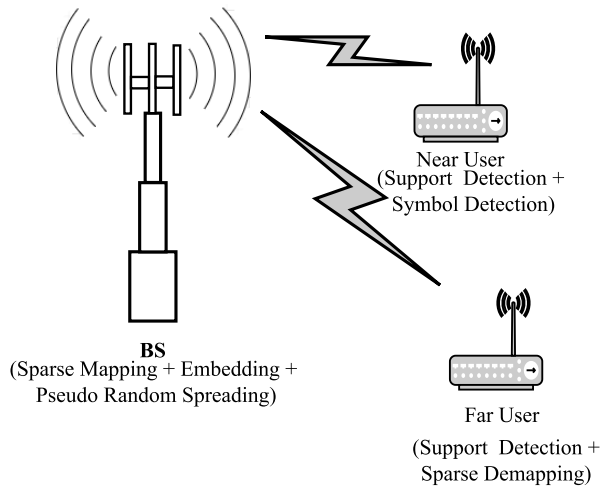


**FIGURE 4.** Downlink MU-SVC system model.

Conversely, NU data is extracted through support detection followed by symbol demodulation. This differentiation in decoding mechanisms enables the separation and recovery of NU and FU data effectively. Moreover, in traditional SVC, when two users transmit data, each requires a separate sparse vector, and both must perform support detection and symbol demodulation. However, in the proposed MU-SVC scheme, only the NU handles both support detection and symbol demodulation, while the FU only needs support detection for data recovery. Moreover, an ultra-short packet can carry multiple symbols instead of just one, enhancing the MU-SVC scheme's efficiency while reducing complexity in multi-user transmissions.

## III. PERFORMANCE ANALYSES OF MU-SVC

In the proposed MU-SVC scheme, it is observed that the non-zero position of the sparse vector corresponds to FU data and embedded symbols in the non-zero position are associated with the NU data. Thus, we study the performance of MU-SVC as two folds viz., PoER and SER, rather than conventional analysis such as BER, BLER, etc. PoER can be defined as the probability of unsuccessful decoding of the exact non-zero positions from the sparse vector. PoER is analyzed for FU as well as NU because both the users need to identify the non-zero position and SER is calculated only for NU which retrieves its information through symbol detection

**TABLE 2. MU-Sparse mapping of users information for $K = 2, U = 2, W = 5, N = 9$.**

| FU Information ($b = 5$ *bits*) | MU-Sparse Vectors ($N = 9$ *bits*) |
|---|---|
| 0 0 0 0 0 | $x_1^{NU}\ x_2^{NU}\ 0\ 0\ 0\ 0\ 0\ 0\ 0$ |
| 0 0 0 0 1 | $x_1^{NU}\ 0\ x_2^{NU}\ 0\ 0\ 0\ 0\ 0\ 0$ |
| 0 0 0 1 0 | $0\ x_1^{NU}\ x_2^{NU}\ 0\ 0\ 0\ 0\ 0\ 0$ |
| 0 0 0 1 1 | $x_1^{NU}\ 0\ 0\ x_2^{NU}\ 0\ 0\ 0\ 0\ 0$ |
| ⋮ | ⋮ |
| 1 1 1 1 1 | $0\ 0\ 0\ x_1^{NU}\ 0\ 0\ 0\ 0\ x_2^{NU}$ |

techniques. However, the PoER corresponding to NU does not impact the performance of NU, since its information is only the symbols. This paper conducts a general analysis of PoER and SER, considering $b$ bits of information, sparse vector length $N$, sparsity $K$, and $m$ physical resources.

### A. SIGNIFICANCE OF POER IN MU-SVC

The decoding of FU and NU information involves the identification of non-zero positions and symbol decoding, respectively. To be precise, the non-zero positions replicate the FU information and symbols represent NU data. Since non-zero position decoding is alone sufficient to obtain the FU information, its performance lies upon the number of errors in decoding the non-zero positions. Thus, PoER calculation is required to analyze the FU performance in the MU-SVC scheme. Table 3 (Refer to Annexure) shows the sparse mapped vectors at the transmitter and demapped sparse vectors with decoded data at the receiver. All possible combinations of 5 bit input data for $K = 2$ with a transmit SNR of $-2$ dB are considered for PoER analysis at the FU. It can be observed that for half of the input data combinations, the sparse demapping is done perfectly without error in decoding the non-zero positions. For the remaining input combinations, the exact identification of the non-zero positions is mismatched and in most cases, only a single position is identified to be the error. Also, the significance of PoER is to study the characteristic of SRA on the MU-SVC scheme concerning the error in decoding the position of non-zero elements. In conventional performance analyses such as BLER, packet error rate (PER), etc., even a single position change detected at the receiver leads to an entire sparse vector being the error, thereby degrading the performance of the system. On the other hand, to obtain the NU data, decoding of symbols embedded at the non-zero positions of the sparse vector is required. However, direct symbol detection could not be possible without the identification of the non-zero positions. Thus, initially, the non-zero position is identified and subsequently symbol decoding is performed to obtain the NU information. Similar to Table 4 analyses at the NU can be performed which contributes to less PoER due to the distance factor from the BS. Finally, the PoER-based performance analysis demonstrates that the MU-SVC scheme provides greater reliability compared to conventional short-packet coding schemes.

### B. POER FOR FU AND NU

We consider the sparsity to be $K$ and the non-zero elements be at the $k$-th and $l$-th position such that $\Omega_s = k,\ l$. Thus, the support (non-zero position) can be defined as $\tilde{\mathbf{s}}_\Omega = \left[\tilde{\mathbf{s}}_k, \tilde{\mathbf{s}}_l\right]^T$ where $\tilde{\mathbf{s}}_k = \mathfrak{A}_k + j\mathfrak{B}_k$ and $\tilde{\mathbf{s}}_l = \mathfrak{A}_l + j\mathfrak{B}_l$, where, $\mathfrak{A}$ and $\mathfrak{B}$ are complex variables. PoER occurs when support is not identified correctly by the SRA and mathematically written as,

$$PoER = P\left(\mathbf{\Omega}_{\tilde{\mathbf{s}}}^* \neq \mathbf{\Omega}_{\tilde{\mathbf{s}}}\right). \tag{8}$$

where $\mathbf{\Omega}_{\tilde{\mathbf{s}}}$ is the exact positions of non-zero elements. OMP performs support detection and the support identified successfully at $p$-th iteration be $I^p$, where $I$ is the probability of success and the corresponding probability can be expressed as,

$$P_{success} = 1 - P\left(\mathbf{\Omega}_{\tilde{\mathbf{s}}}^* \neq \mathbf{\Omega}_{\tilde{\mathbf{s}}}\right) = P\left(I^2 \middle| I^1\right) P\left(I^1\right). \tag{9}$$

The NU data is converted to symbols through any type of modulation schemes and the real and imaginary part decisions are taken in first and second iteration, respectively. The conditional probability for identifying the support in first iteration with channel coefficients $\mathbf{h_{FU}} = [\mathbf{h}_1, \mathbf{h}_2, \ldots \mathbf{h}_m]^T$ is given by,

$$\begin{aligned} P\left(I^1 | \mathbf{h_{FU}}\right) &= \prod_{(i=1,\ i\neq k)}^{N} P\left(\left|\mathfrak{A}\left\langle \frac{\boldsymbol{\phi}_k}{\|\boldsymbol{\phi}_k\|_2}, r^0 \right\rangle\right|\right) \\ &\geq P\left(\left|\mathfrak{A}\left\langle \frac{\boldsymbol{\phi}_i}{\|\boldsymbol{\phi}_i\|_2}, r^0 \right\rangle\right|\right), \end{aligned} \tag{10}$$

where, $r^0$ is the initial residual factor. The support estimate at the first iteration is expressed as,

$$\begin{aligned} \mathfrak{A}\left\langle \frac{\boldsymbol{\phi}_k}{\|\boldsymbol{\phi}_k\|_2}, r^0 \right\rangle &= \mathfrak{A}\left\langle \frac{\boldsymbol{\phi}_k}{\|\boldsymbol{\phi}_k\|_2}, \boldsymbol{\phi}_k\tilde{\mathbf{s}}_k + \boldsymbol{\phi}_l\tilde{\mathbf{s}}_l + \boldsymbol{\nu} \right\rangle \\ &= \mathfrak{A}_k \|\mathbf{h_{FU}}\|_2 + \mathfrak{A}_l\mu_{kl} \|\mathbf{h_{FU}}\|_2 + \mathbf{z}_r. \end{aligned} \tag{11}$$

The term $\mu_{kl}$ mutual coherence is the maximum correlation between $\mathbf{c}_k$ and $\mathbf{c}_l$, where $\mathbf{c}_k$ and $\mathbf{c}_l$ are code book vector at $k$-th and $l$-th estimates. The terms $\mathfrak{A}_k$ and $\mathfrak{A}_l$ are the real part variables at $k$-th and $l$-th estimates, $\mathbf{z}_r = \mathfrak{A}\left(\frac{\boldsymbol{\phi}_k^T}{\|\boldsymbol{\phi}_k\|_2}\boldsymbol{\nu}\right)$. We have

$$\mathfrak{A}\left\langle \frac{\boldsymbol{\phi}_i}{\|\boldsymbol{\phi}_i\|_2}, r^0 \right\rangle = \mathfrak{A}_k\mu_{ik} \|\mathbf{h_{FU}}\|_2 + \mathfrak{A}_l\mu_{il} \|\mathbf{h_{FU}}\|_2 + \mathbf{z}_i. \tag{12}$$

where, $\mathbf{z}_i = \mathfrak{A}\left(\frac{\boldsymbol{\phi}_i^T}{\|\boldsymbol{\phi}_i\|_2}\boldsymbol{\nu}\right)$. Now, utilising $P\left(|A| \geq |B|\right) = P\left(A > |B|\right)P\left(A > 0\right) + P\left(-A > |B|\right)P\left(A < 0\right)$ in (11)

and (12), the conditional probability of the estimate is given by,

$$P\left(\left|\mathfrak{A}\left\langle\frac{\boldsymbol{\phi}_k}{\|\boldsymbol{\phi}_k\|_2}, r^0\right\rangle\right| \geq \left|\mathfrak{A}\left\langle\frac{\boldsymbol{\phi}_i}{\|\boldsymbol{\phi}_i\|_2}, r^0\right\rangle\right|\right) = P\left(\left|\left(\mathfrak{A}_k + \mathfrak{A}_l\mu_{kl}\right)\|\mathbf{h_{FU}}\|_2 + \mathbf{z}_r\right| \geq \left|\left(\mathfrak{A}_k\mu_{ik} + \mathfrak{A}_l\mu_{il}\right)\|\mathbf{h_{FU}}\|_2 + \mathbf{z}_i\right|\right). \quad (13)$$

The $Q$ function criteria, $P(\mathbf{z}_k < -\|\mathbf{h}\|_2) = 1 - Q\left(-\frac{\|\mathbf{h}\|_2}{\frac{\sigma_\nu}{\sqrt{2}}}\right) \geq 1 - exp\left(-\frac{\|\mathbf{h}\|_2^2}{\sigma_\nu^2}\right)$ is used for further simplification of (13) and the support estimate is rewritten as,

$$P\left(\left|\mathfrak{A}\left\langle\frac{\boldsymbol{\phi}_k}{\|\boldsymbol{\phi}_k\|_2}, r^0\right\rangle\right|\right) \geq 1 - exp\left(-\frac{\|\mathbf{h_{FU}}\|_2^2\,\zeta_1}{2\sigma_\nu^2}\right) - exp\left(-\frac{\|\mathbf{h_{FU}}\|_2^2\,\eta_1}{\sigma_\nu^2}\right), \quad (14)$$

where, $\sigma_\nu^2$ is the noise variance, $\zeta_1 = \{\mathfrak{A}_k + \mathfrak{A}_l\mu^* - (|\mathfrak{A}_k| + |\mathfrak{A}_l|)\,\mu^*\}^2$ and $\eta_1 = \{\mathfrak{A}_k + \mathfrak{A}_l\mu^*\}^2$ in which $\mu^*$ is the absolute value of the maximum correlation between two columns of $\boldsymbol{\phi}$. Furthermore, the probability of support at the first iteration with realization of FU channel gain is expressed as,

$$P\left(I^1\right) = \int P\left(I^1|\mathbf{h_{FU}}\right) f_{\mathbf{h_{FU}}}(x)\,dx = E_h\left[P\left(I^1|\mathbf{h_{FU}}\right)\right]. \quad (15)$$

On simplification, by $E_h\left[exp\left(-\frac{\|\mathbf{h_{FU}}\|_2^2}{\sigma_\nu^2}\right)\middle|\mathbf{h_{FU}}\right] = \left(1 + \frac{1}{\sigma_\nu^2}\right)^{-m}$ [6], where $E_h$ is the expectation with respect to FU channel realization. The first iteration support estimate is expressed as,

$$P\left(I^1\right) \geq \left(1 - \left(1 + \frac{\zeta_1}{2\sigma_\nu^2}\right)^{-m} - \left(1 + \frac{\eta_1}{\sigma_\nu^2}\right)^{-m}\right)^{N-1}. \quad (16)$$

Similarly, the success of second iteration can be derived and expressed as,

$$P\left(I^2\right) \geq \left(1 - \left(1 + \frac{\zeta_2}{2\sigma_\nu^2}\right)^{-m} - \left(1 + \frac{\eta_2}{\sigma_\nu^2}\right)^{-m}\right)^{N-2}, \quad (17)$$

where $\zeta_2 = \{\mathfrak{B}_l - |\mathfrak{B}_l|\,\mu^*\}^2$ and $\eta_2 = \mathfrak{B}_l^2$. Finally, the closed form expression of PoER for both the iteration can be written as,

$$PoER_{FU} \geq 1 - \left(1 - \left(1 + \frac{\zeta_1}{2\sigma_\nu^2}\right)^{-m} - \left(1 + \frac{\eta_1}{\sigma_\nu^2}\right)^{-m}\right)^{N-1} \times \left(1 - \left(1 + \frac{\zeta_2}{2\sigma_\nu^2}\right)^{-m} - \left(1 + \frac{\eta_2}{\sigma_\nu^2}\right)^{-m}\right)^{N-2}. \quad (18)$$

The PoER of the NU is same as that of FU with the only difference being realization of the NU channel gain ($\mathbf{h_{NU}}$).

### C. SER FOR NU

The NU adopts symbol detection techniques to decode its information and SER occurs if the detected symbol is incorrect. Assuming the transmitted symbol to be $\tilde{\mathbf{S}}_k$ and incorrect symbol as $\tilde{\mathbf{S}}_{\tilde{k}}$, the pair wise error probability is expressed in terms of $Q$ function [39] as,

$$P\left(\tilde{\mathbf{s}}_k \to \tilde{\mathbf{s}}_{\tilde{k}}|y, \mathbf{h_{NU}}\right) = Q\left(\sqrt{\frac{\left\|\boldsymbol{\phi}_i\left(\tilde{\mathbf{s}}^k - \tilde{\mathbf{s}}^l\right)\right\|^2}{2\sigma_\nu^2}}\right). \quad (19)$$

Now, the channel is realized and minimum Euclidean distance ($d_{min}$) among the symbols are considered with NU channel gain. Using $Q(x) \leq exp(-\frac{x^2}{2})$, (15) can be simplified and written as,

$$SER_{NU} \leq k\left(1 + \frac{\mu^* d_{min}^2}{4\sigma_\nu^2}\right)^{-m}. \quad (20)$$

Thus, the final expression for SER at NU has been obtained in which the resource allocation plays a vital role in deciding the SER performance. The numerical expressions of PoER and SER are validated with Monte Carlo simulation over Rayleigh fading channel in the next section and the performance of the MU-SVC scheme is analyzed with various key parameters.

### D. BER FOR MU-SVC AND ESVC

The BER analysis is performed to enact the performance gain of MU-SVC over the ESVC scheme. Since PoER analysis is not applicable to conventional SVC and ESVC techniques (due to the absence of NU and FU segregation, as well as the use of universal encoding and decoding techniques for the transmitter and receiver), BER is calculated to contrast the performance of the proposed scheme. The BER can be analyzed similarly to BLER in [9]. It is defined as the number of bits received as an error in the total number of bits transmitted. The probability of unsuccessful decoding can be obtained by $BER = 1 - P_{success}$ for both FU and NU with their respective channel coefficients (The step-by-step numerical analysis is omitted, as BER analysis is traditional, and the primary focus and uniqueness of this paper lie in PoER analysis). In the case of ESVC, both the users need to perform support detection as well as symbol decoding to decode their information. To calculate BER, the

detected symbols are converted to bits. On the other hand in MU-SVC, the FU performs only support detection to decode its information from the non-zero positions, whereas, NU is concerned only with symbol decoding. The BER performance for the MU-SVC and ESVC schemes are traced out in Section IV.

### E. COMPLEXITY ANALYSIS

The complexity analysis is performed by considering the process of decoding the non-zero positions and symbols as $\rho_p$ and $\rho_{SD}$ respectively, for ultra-short packet transmission. In the case of ESVC, the support identification ($\rho_p$) and symbol decoding ($\rho_{SD}$) has to be done by each user individually to obtain their information. Whereas in the proposed scheme, the FU performs only support identification ($\rho_p$) and the NU undergoes both processes ($\rho_p + \rho_{SD}$). Thus, the complexity at the NU for the proposed MU-SVC is the operation of $(U \times (IKN + S_K))$. Likewise, the complexity at the FU is only to detect the non-zero position which is $U \times (IKN)$, where $I$ is the number of iteration SRA takes for convergence, $U$ is the number of users and $S_K$ is the $K$ number of symbol detection process. Thus, as a system, the complexity of the proposed MU-SVC lies in performing the operation of $U \times ((IKN)^2 + S_K)$. Whereas, in ESVC complexity lies in detecting the non-zero positions and decoding the symbols for each user which is $U \times (IKN + S_K)$. Similarly, in case of SVC the complexity is to detect the non-zero positions alone i.e., $U \times (IKN)$. Even though it seems that the complexity of SVC is less than MU-SVC, the amount of information transmitted, number of users served and reliability are much higher with less latency than former. Table 4 shows the complexity analyses for MU-SVC and ESVC schemes for the MU environment in terms of decoding at the user end. Inference shows that the MU-SVC requires less computation, thereby achieving less complexity with reduced latency than the ESVC scheme.

### F. SPECTRAL OCCUPANCY

The spectral occupancy is computed in terms of time slots required for users to make successful communication. Without loss of generality, the time duration is considered as a slot without specifying a fixed length. Fig. 5 shows the spectral occupancy for SVC, ESVC and MU-SVC schemes, in the MU environment. For ultra-short packet transmission, the SVC and ESVC requires individual time slots to serve each user, whereas, MU-SVC serves more than one user simultaneously in a single time frame. Thus, the proposed MU-SVC scheme is spectral efficient and serves more users simultaneously than ESVC and SVC schemes.

## IV. RESULTS AND DISCUSSIONS

In this section, the key results are presented for MU-SVC in terms of transmitting SNR versus PoER and SER. For simulation, the parameters are assigned to $N = 96, b = 5, m = 88, K = 2, \mu^* \approx 0.6$ and the distance of FU is twice as that of NU. In Fig. 6, the performance in terms of

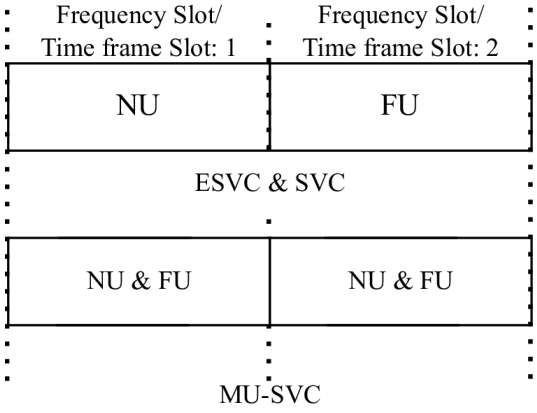


**FIGURE 5.** Spectral occupancy of existing SVC schemes and MU-SVC.

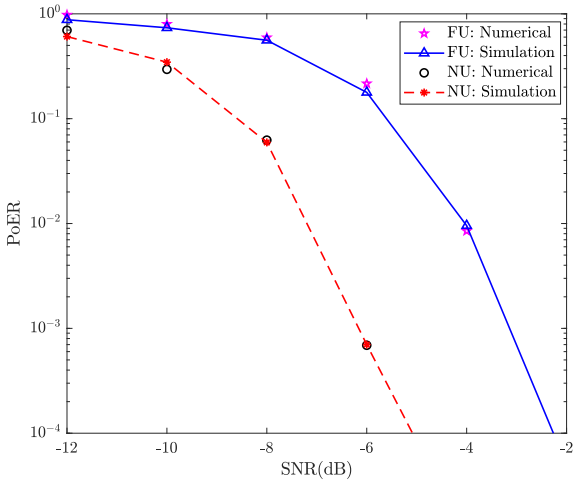


**FIGURE 6.** PoER MC simulation and numerical validation of MU-SVC.

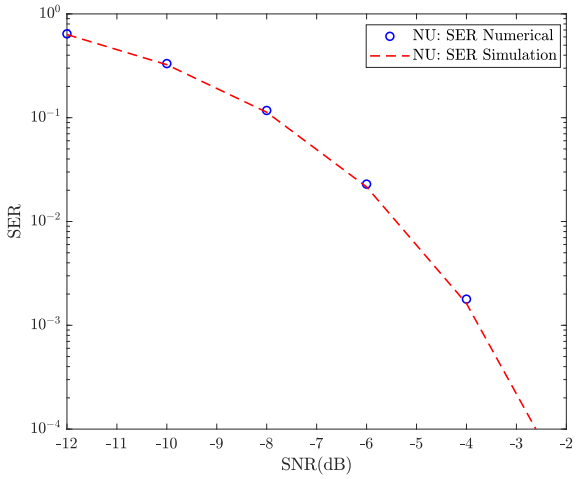


**FIGURE 7.** MU-SVC SER performance of NU with numerical validation.

PoER for FU and NU is traced out with the upper bound. It is observed that NU performs better than FU due to the distance factor and on an average 2 $dB$ gain is obtained by

**TABLE 3.** Significance of PoER in MU-Sparse mapping of users information for $K = 2$, $U = 2$, $W = 5$, $SNR = -2$ $dB$.

| Data | Sparse Mapping | Support Detection | Sparse Demapping | No. of error in position | No. of errors in bits |
|---|---|---|---|---|---|
| 00000 | 1100000000 | 0100000100 | 10000 | 1 | 1 |
| 00001 | 1010000000 | 1010000000 | 00001 | 0 | 0 |
| 00010 | 0110000000 | 0101000000 | 00100 | 1 | 2 |
| 00011 | 1001000000 | 1000100000 | 00110 | 1 | 1 |
| 00100 | 0101000000 | 0000011000 | 10100 | 2 | 1 |
| 00101 | 0011000000 | 0011000000 | 00101 | 0 | 0 |
| 00110 | 1000100000 | 0000110000 | 01110 | 1 | 1 |
| 00111 | 0100100000 | 0100001000 | 01011 | 1 | 2 |
| 01000 | 0010100000 | 0010100000 | 01000 | 0 | 0 |
| 01001 | 0001100000 | 0001100000 | 01001 | 0 | 0 |
| 01010 | 1000010000 | 1000000100 | 01111 | 1 | 2 |
| 01011 | 0100010000 | 0000010100 | 11010 | 1 | 2 |
| 01100 | 0010010000 | 0010010000 | 01100 | 0 | 0 |
| 01101 | 0001010000 | 0001000010 | 11000 | 1 | 3 |
| 01110 | 0000110000 | 0000110000 | 01110 | 0 | 0 |
| 01111 | 1000000100 | 1000000100 | 01111 | 0 | 0 |
| 10000 | 0100000100 | 0000101000 | 10011 | 2 | 2 |
| 10001 | 0010000100 | 0010000100 | 10001 | 0 | 0 |
| 10010 | 0001001000 | 0001001000 | 10010 | 0 | 0 |
| 10011 | 0000101000 | 0000101000 | 10011 | 0 | 0 |
| 10100 | 0000011000 | 0000101000 | 10011 | 1 | 3 |
| 10101 | 1000000010 | 1000000001 | 11100 | 1 | 2 |
| 10110 | 0100000010 | 0100000010 | 10110 | 0 | 0 |
| 10111 | 0010000010 | 1000100000 | 00110 | 2 | 2 |
| 11000 | 0001000010 | 1000000010 | 10101 | 1 | 3 |
| 11001 | 0000100010 | 0000100010 | 11001 | 0 | 0 |
| 11010 | 0000010010 | 0000010010 | 11010 | 0 | 0 |
| 11011 | 0000001100 | 0000001100 | 11011 | 0 | 0 |
| 11100 | 1000000001 | 1000000010 | 10101 | 1 | 2 |
| 11101 | 0100000001 | 0100001000 | 01011 | 1 | 3 |
| 11110 | 0010000001 | 0010000001 | 11110 | 0 | 0 |
| 11111 | 0001000001 | 0010000010 | 10111 | 2 | 1 |

NU when compared with FU to achieve a PoER greater than $10^{-2}$. Also, the simulation result well matches with upper bound analytical values. Further, it is evident that the system is very reliable even at low SNR values due to the sparse

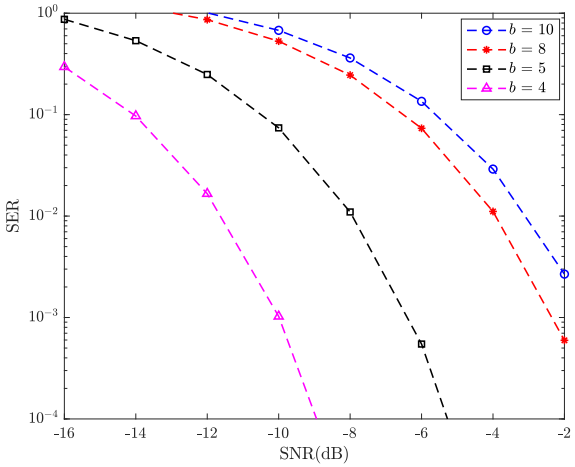


**FIGURE 8.** MU-SVC SER for NU with various information bits.

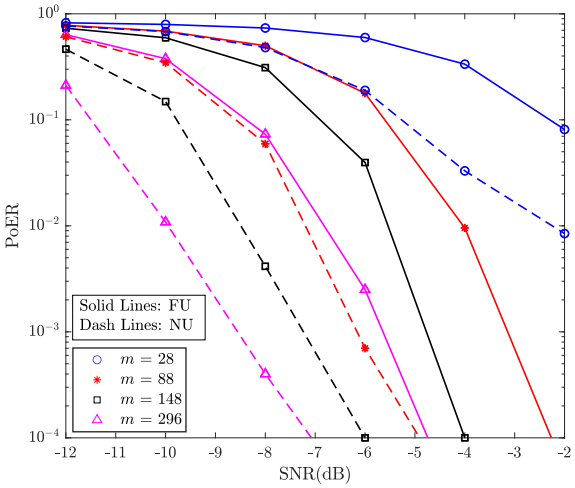


**FIGURE 9.** MU-SVC PoER performance with various resource allocation.

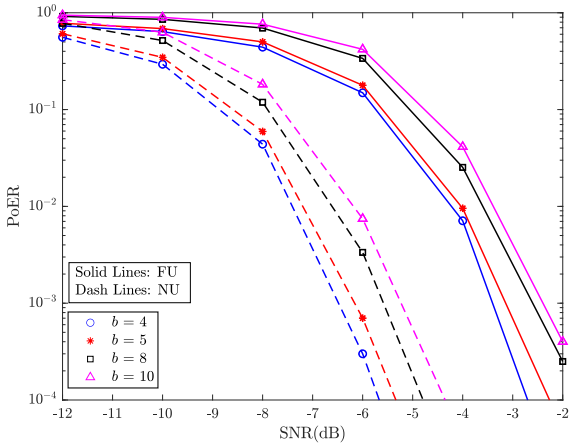


**FIGURE 10.** MU-SVC PoER performance with various information bits.

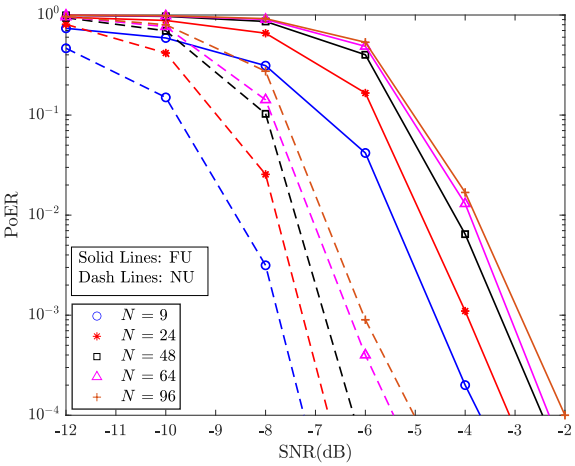


**FIGURE 11.** MU-SVC PoER performance with various sparse vector length.

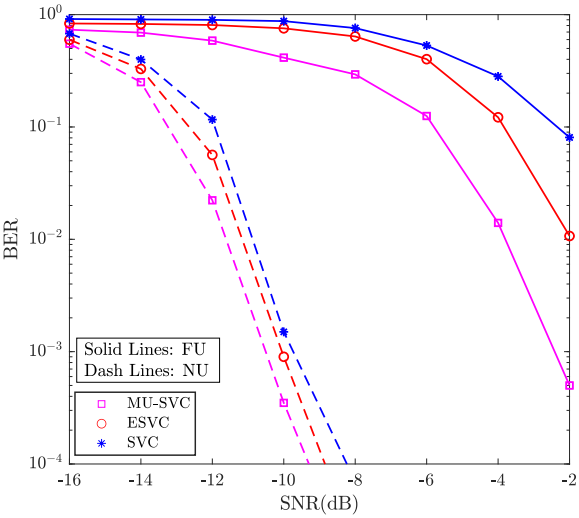


**FIGURE 12.** BER performance of MU-SVC with existing SVC schemes.

nature of the information and CS-based decoding techniques. The NU performs symbol detection in addition to support identification and its analyses is shown in Figs. 7 and 8. The simulation values are evaluated with numerical in Fig. 7 and observed that as SNR increases the SER attained is low which means the probability of symbol decoding success is high. Furthermore, SER for various input information bits is analyzed in Fig. 8 which shows that the SER and number of information are directly proportional to each other. This is because as the amount of information to be encoded is more, the length of the sparse vector gets increased which leads to a higher decoding error.

The PoER performance analysis of FU and NU with various resource allocations ($m = 28, 88, 148, 296$) is shown in Fig. 9 with $N = 320$. Observations indicate that as the number of resources or the sensing matrix size increases, PoER decreases due to the availability of sufficient measurements for accurate symbol decoding. To be precise, if the measurement changes from 28 to 88, a gain of 3 *dB* and 4 *dB* in FU and NU, respectively are obtained. Moreover, it is observed that the reliability of the MU-SVC scheme is very high, and low latency can be achieved with less iteration.

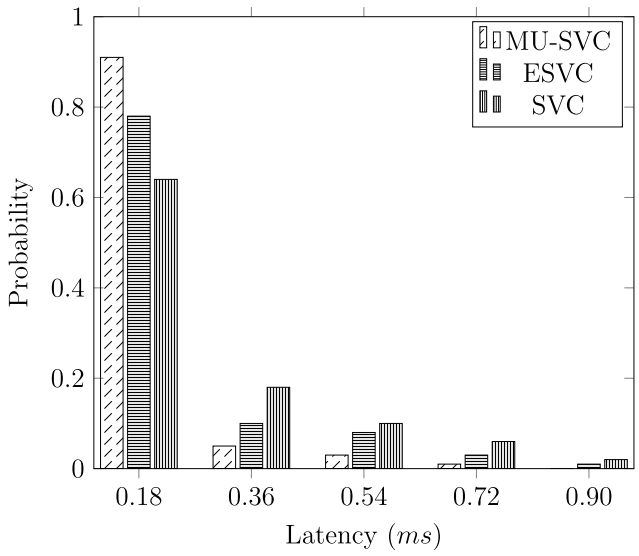


**FIGURE 13.** Probability of Transmission Latency of existing SVC schemes and MU-SVC (BER = $10^{-6}$).

In Fig. 10, the SNR versus PoER plot for various input information bits ($b = 4, 5, 8, 10$) is analyzed for FU and NU over the Rayleigh fading channel. Investigation shows if the input information is increased for the same amount of measurements, the performance of the MU-SVC scheme is poor for both the users. Thus, as $b$ increases, performance can improve if bandwidth constraints are relaxed. Since the sparsity is high (less number of non-zero elements), support is identified in less iteration through greedy algorithms. Also, it is evident that the input bits and PoER are proportional to each other with a fixed resource.

The performance of MU-SVC concerning various sparse vector size ($N = 9, 24, 48, 64, 96$) are analyzed and plotted in Fig. 11. From the result, it is clear that the error rate depends on sparse vector size for a specific measurement but the performance is not affected as in case of varying the resource. As $N$ gets high, there is a marginal difference in PoER for FU as well as NU. Finally, MU-SVC scheme provides ultra-reliability even in a very low SNR regime due to the sparse nature of the information transmitted. Also, decoding involves only position identification and support with symbol detection for FU and NU, respectively. Thus, MU-SVC provides low latency with less system complexity in MU scenario.

Fig. 12 traces the BER plot of MU-SVC with ESVC and SVC schemes for various transmit SNR with $K = 2, m = 5, N = 10$. Immediate inference is that for all the schemes BER decreases as SNR gets high and the FU performance is comparatively less than NU due to the distance factor. Keen observation discloses that the performance of MU-SVC is superior to ESVC and SVC for both the users. In MU-SVC, the FU performs only support identification to decode its information and thus possesses a gain of 2 $dB$ for BER of $10^{-3}$ over the ESVC scheme which requires support identification as well as symbol detection. In the case of NU, both the schemes perform support identification and symbol detection to decode their information, but the NU of the MU-SVC shows less BER. This is because the information of NU depends only on the symbols and not on non-zero positions, and hence the support identification error is neglected. In case of SVC, the performance depends on decoding of non-zero positions alone, yet its error rate is higher than ESVC and MU-SVC. This is due to the symbol decoding process, which contributes for less error than position decoding. Thus, the MU-SVC provides user fairness and more efficient than ESVC and SVC schemes in MU scenario.

**TABLE 4.** Complexity analysis.

| User | ESVC | MU-SVC |
|---|---|---|
| NU | $\rho_p + \rho_{SD}$ | $\rho_p + \rho_{SD}$ |
| | $IKN + S_K$ | $IKN + S_K$ |
| FU | $\rho_p + \rho_{SD}$ | $\rho_p$ |
| | $IKN + S_K$ | $IKN$ |

Finally, the transmission latency is evaluated for the proposed MU-SVC scheme and compared with the ESVC and SVC schemes (excluding processing, queuing, and propagation delays). The simulation setup considers a system with $N = 96$, $b = 5$, $m = 88$, $K = 2$, and $U = 2$. The transmit SNR is set to $-2$ dB, and the target error rate is $10^{-6}$. The optimal power allocation factor is set as $\mu^* \approx 0.6$. The analysis is conducted under a re-transmission (repetition) scheme, ensuring that both NU and FU data undergo repeated transmission until successful decoding. Fig. 13 illustrates the probability distribution of transmission latency for the MU-SVC, ESVC, and SVC schemes. The results indicate that the proposed MU-SVC scheme achieves significantly lower latency compared to conventional schemes–on average, 15% lower than ESVC and 34% lower than SVC. This reduction is attributed to the fact that in ESVC and SVC schemes, both users must perform support detection and symbol decoding, which introduces additional delay. Additionally, the proposed MU-SVC scheme successfully decodes the information within 1 ms, thereby meeting the stringent latency requirements of xURLLC while maintaining spectral efficiency, making it suitable for B5G.

## V. CONCLUSION

In this paper, we proposed a novel MU-SVC scheme, for the transmission of ultra-short packets in xURLLC that aids for time critical and reliable systems. The FU information is mapped into a sparse vector and the NU information are converted into symbols and embedded into the non-zero position of the FU sparse vector. The decoding of the sparse vector is done through SRA and sparse demapping in FU, whereas SRA with symbol detection technique is adopted in NU. From the numerical and simulation results of PoER

and SER, it is demonstrated that our proposed MU-SVC scheme achieves the reliability and latency standards of B5G at the low SNR regime itself. The MU-SVC performance is analyzed by varying the key parameters and it is proved that the proposed scheme serves multiple users without sacrificing the reliability standard. Also, the significance of PoER performance in MU-SVC is elaborated for the FU. Furthermore, BER, complexity, and latency analyses with spectral occupancy proves that the proposed MU-SVC outperforms the SVC and ESVC schemes. Thus, the proposed MU-SVC scheme is shown to be a strong candidate for xURLLC scenarios with high spectral efficiency for ultra-short packet transmission in B5G applications.

## ANNEXURE

See Table 3.

## REFERENCES

[1] J. Sachs, G. Wikstrom, T. Dudda, R. Baldemair, and K. Kittichokechai, "5G radio network design for ultra-reliable low-latency communication," *IEEE Netw.*, vol. 32, no. 2, pp. 24–31, Mar. 2018.

[2] H. Chen, R. Abbas, P. Cheng, M. Shirvanimoghaddam, W. Hardjawana, W. Bao, Y. Li, and B. Vucetic, "Ultra-reliable low latency cellular networks: Use cases, challenges and approaches," *IEEE Commun. Mag.*, vol. 56, no. 12, pp. 119–125, Dec. 2018.

[3] G. J. Sutton, J. Zeng, R. P. Liu, W. Ni, D. N. Nguyen, B. A. Jayawickrama, X. Huang, M. Abolhasan, Z. Zhang, E. Dutkiewicz, and T. Lv, "Enabling technologies for ultra-reliable and low latency communications: From PHY and MAC layer perspectives," *IEEE Commun. Surveys Tuts.*, vol. 21, no. 3, pp. 2488–2524, 3rd Quart., 2019.

[4] C. Pan, Z. Wang, H. Liao, Z. Zhou, X. Wang, M. Tariq, and S. Al-Otaibi, "Asynchronous federated deep reinforcement learning-based URLLC-aware computation offloading in space-assisted vehicular networks," *IEEE Trans. Intell. Transp. Syst.*, vol. 24, no. 7, pp. 7377–7389, Jul. 2023.

[5] A. Dalgkitsis, L. A. Garrido, F. Rezazadeh, H. Chergui, K. Ramantas, J. S. Vardakas, and C. Verikoukis, "SCHE2MA: Scalable, energy-aware, multidomain orchestration for beyond-5G URLLC services," *IEEE Trans. Intell. Transp. Syst.*, vol. 24, no. 7, pp. 7653–7663, Jul. 2023.

[6] T.-K. Le, U. Salim, and F. Kaltenberger, "Improving ultra-reliable low-latency communication in multiplexing with enhanced mobile broadband in grant-free resources," in *Proc. IEEE 30th Annu. Int. Symp. Pers., Indoor Mobile Radio Commun. (PIMRC)*, Sep. 2019, pp. 1–6.

[7] P. Popovski, C. Stefanovic, J. J. Nielsen, E. de Carvalho, M. Angjelichinoski, K. F. Trillingsgaard, and A.-S. Bana, "Wireless access in ultra-reliable low-latency communication (URLLC)," *IEEE Trans. Commun.*, vol. 67, no. 8, pp. 5783–5801, Aug. 2019.

[8] T. Yoshizawa, S. B. M. Baskaran, and A. Kunz, "Overview of 5G URLLC system and security aspects in 3GPP," in *Proc. IEEE Conf. Standards Commun. Netw. (CSCN)*, Oct. 2019, pp. 1–5.

[9] S. R. Pokhrel, J. Ding, J. Park, O.-S. Park, and J. Choi, "Towards enabling critical mMTC: A review of URLLC within mMTC," *IEEE Access*, vol. 8, pp. 131796–131813, 2020.

[10] R. Ali, Y. B. Zikria, A. K. Bashir, S. Garg, and H. S. Kim, "URLLC for 5G and beyond: Requirements, enabling incumbent technologies and network intelligence," *IEEE Access*, vol. 9, pp. 67064–67095, 2021.

[11] T.-K. Le, U. Salim, and F. Kaltenberger, "An overview of physical layer design for ultra-reliable low-latency communications in 3GPP releases 15, 16, and 17," *IEEE Access*, vol. 9, pp. 433–444, 2021.

[12] H. Ji, S. Park, and B. Shim, "Sparse vector coding for 5G ultra-reliable and low latency communications," in *Proc. IEEE Int. Conf. Commun. (ICC)*, May 2018, pp. 1–6.

[13] H. Ji, S. Park, and B. Shim, "Sparse vector coding for ultra reliable and low latency communications," *IEEE Trans. Wireless Commun.*, vol. 17, no. 10, pp. 6693–6706, Oct. 2018.

[14] H. Ji, S. Kim, and B. Shim, "Sparse vector coding for ultra short packet transmission," in *Proc. Inf. Theory Appl. Workshop (ITA)*, Feb. 2018, pp. 1–9.

[15] H. Ji and B. Shim, "Sparse vector coding for short packet transmission in massive machine type communications," in *Proc. 24th Asia–Pacific Conf. Commun. (APCC)*, Nov. 2018, pp. 137–140.

[16] T. V. Prabhakar, V. Hemanth, S. Kumar, K. P. Soman, and A. Soman, "Comparative study of recent compressed sensing methodologies in astronomical images," in *Proc. Int. Conf. Eco-Friendly Comput. Commun. Syst.* Cham, Switzerland: Springer, Jan. 2012, pp. 108–116.

[17] K. Narayanankutty, K. Soman, and A. V. Vidyapeetham, "Understanding theory behind compressed sensing," *Int. J. Sens., Comput. Control*, vol. 1, no. 2, pp. 80–91, 2011.

[18] H. Ji, W. Kim, and B. Shim, "Pilot-less sparse vector coding for short packet transmission," *IEEE Wireless Commun. Lett.*, vol. 8, no. 4, pp. 1036–1039, Aug. 2019.

[19] J. Wu, W. Kim, and B. Shim, "Pilot-less one-shot sparse coding for short packet-based machine-type communications," *IEEE Trans. Veh. Technol.*, vol. 69, no. 8, pp. 9117–9120, Aug. 2020.

[20] W. Kim, S. K. Bandari, and B. Shim, "Enhanced sparse vector coding for ultra-reliable and low latency communications," *IEEE Trans. Veh. Technol.*, vol. 69, no. 5, pp. 5698–5702, May 2020.

[21] R. Zhang, B. Shim, Y. Lou, S. Jia, and W. Wu, "Sparse vector coding aided ultra-reliable and low-latency communications in multi-user massive MIMO systems," *IEEE Trans. Veh. Technol.*, vol. 70, no. 1, pp. 1019–1024, Jan. 2021.

[22] X. Zhang, L. Yang, Z. Ding, J. Song, Y. Zhai, and D. Zhang, "Sparse vector coding-based multi-carrier NOMA for in-home health networks," *IEEE J. Sel. Areas Commun.*, vol. 39, no. 2, pp. 325–337, Feb. 2021.

[23] G. Qin, H. Chen, X. Zhang, T. Sato, and D. Zhang, "Uniquely decomposable constellation group-based sparse vector coding for short packet communications," in *Proc. IEEE 94th Veh. Technol. Conf. (VTC-Fall)*, Sep. 2021, pp. 1–5.

[24] X. Zhang, G. Han, D. Zhang, B. Shim, and D. Zhang, "Sparse vector coding-based superimposed transmission for short packet URLLC," in *Proc. IEEE Wireless Commun. Netw. Conf. Workshops (WCNCW)*, Mar. 2021, pp. 1–6.

[25] S. K. Bandari and C. V. R. Rao, "Enhanced sparse vector coding with limited pilot overhead for short packet transmission," in *Proc. Adv. Commun. Technol. Signal Process. (ACTS)*, Dec. 2021, pp. 1–5.

[26] A. Awasthi, M. Kumar, S. K. Bandari, and V. V. Mani, "Maximal ratio sparse vector coding for short packet transmission," in *Proc. IEEE Int. Conf. Adv. Netw. Telecommun. Syst. (ANTS)*, Dec. 2021, pp. 1–4.

[27] X. Zhang, D. Zhang, B. Shim, G. Han, D. Zhang, and T. Sato, "Sparse superimposed coding for short-packet URLLC," *IEEE Internet Things J.*, vol. 9, no. 7, pp. 5275–5289, Apr. 2022.

[28] R. Zhang, B. Shim, W. Yuan, M. D. Renzo, X. Dang, and W. Wu, "Integrated sensing and communication waveform design with sparse vector coding: Low sidelobes and ultra reliability," *IEEE Trans. Veh. Technol.*, vol. 71, no. 4, pp. 4489–4494, Apr. 2022.

[29] L. Yang and P. Fan, "Improved sparse vector code based on optimized spreading matrix for short-packet in URLLC," *IEEE Wireless Commun. Lett.*, vol. 12, no. 4, pp. 728–732, Apr. 2023.

[30] S. Sabapathy, S. Maruthu, L. S. Kumar, and D. N. K. Jayakody, "Outage analysis of sparse vector coding based downlink multicarrier NOMA for URLLC," *IEEE Internet Things J.*, vol. 10, no. 14, pp. 12393–12400, Jun. 2023.

[31] Y. Zhang, X. Zhu, Y. Liu, Y. Jiang, Y. L. Guan, G. D. González, and V. K. N. Lau, "Sparse superimposed vector transmission for short-packet high-mobility communication," *IEEE Wireless Commun. Lett.*, vol. 12, no. 11, pp. 1961–1965, Nov. 2023.

[32] S. Sabapathy, S. Maruthu, and D. N. K. Jayakody, "Rate-splitting sparse vector code for next-generation URLLC systems," *IEEE Wireless Commun. Lett.*, vol. 13, no. 7, pp. 1993–1997, Jul. 2024.

[33] Z. Yang, M. Chen, K.-K. Wong, H. V. Poor, and S. Cui, "Federated learning for 6G: Applications, challenges, and opportunities," *Engineering*, vol. 8, pp. 33–41, Jan. 2022. [Online]. Available: https://www.sciencedirect.com/science/article/pii/S2095809921005245

[34] G. Zhu, Z. Lyu, X. Jiao, P. Liu, M. Chen, J. Xu, S. Cui, and P. Zhang, "Pushing AI to wireless network edge: An overview on integrated sensing, communication, and computation towards 6G," *Sci. China Inf. Sci.*, vol. 66, no. 3, Mar. 2023, Art. no. 130301.

[35] Y. Yang et al., "6G network AI architecture for everyone-centric customized services," 2022, *arXiv:2205.09944*.

[36] A. Zubow, P. Gawłowicz, and F. Dressler, "Less is more: Towards low-latency communication trough cross-technology communication," in *Proc. 17th ACM Workshop Mobility Evolving Internet Archit.*, Oct. 2022, pp. 55–60.
[37] K. Lakshmi, P. Muralikrishna, and K. P. Soman, "Compressive estimation of UWA channels for OFDM transmission using iterative sparse reconstruction algorithms," in *Proc. Int. Mutli-Conf. Autom., Comput., Commun., Control Compressed Sens. (iMac4s)*, Mar. 2013, pp. 847–851.
[38] S. Ravindranath, S. R. N. Ram, S. Subhashini, A. V. S. Reddy, M. Janarth, R. AswathVignesh, R. Gandhiraj, and K. P. Soman, "Compressive sensing based image acquisition and reconstruction analysis," in *Proc. Int. Conf. Green Comput. Commun. Electr. Eng. (ICGCCEE)*, Mar. 2014, pp. 1–6.
[39] G. Karagiannidis and A. Lioumpas, "An improved approximation for the Gaussian Q-function," *IEEE Commun. Lett.*, vol. 11, no. 8, pp. 644–646, Aug. 2007.

**SUNDARESAN SABAPATHY** (Member, IEEE) received the B.Tech. degree in ECE from Pondicherry University, Puducherry, the M.Tech. degree in remote sensing and wireless sensor networks from Amrita Vishwa Vidyapeetham, Coimbatore, and the Ph.D. degree in wireless communications from the National Institute of Technology Puducherry. He is currently an Assistant Professor with the School of Artificial Intelligence, Amrita Vishwa Vidyapeetham. He has five years of teaching experience and has published various research articles and book chapters in reputed journals and international conferences. He also serves as a Reviewer for IEEE TRANSACTIONS ON VEHICULAR TECHNOLOGY, IEEE INTERNET OF THINGS JOURNAL, IEEE LATIN AMERICA TRANSACTIONS, *Digital Signal Processing* journal (Elsevier), *Internet Technology Letters* (Wiley), *Advances in Science, Technology and Engineering Systems Journal* (ASTESJ), *Journal of Engineering Research and Science*, and *International Journal of Innovative Research in Engineering & Multidisciplinary Physical Sciences*. His research interests include URLLC, PHY layer design, 5G and beyond systems, software defined radio, and deep learning.

**SURENDAR MARUTHU** (Member, IEEE) received the B.E. and M.Tech. degrees in ECE from the Thiagarajar College of Engineering, Madurai, and the Ph.D. degree in ECE from the National Institute of Technology, Thiruchirapalli. He is currently an Assistant Professor with the Department of Electronics and communication engineering, NIT Puducherry. Since 2018, he has been an Assistant Professor with the Department of Electronics and Communication Engineering, National Institute of Technology Puducherry, Puducherry, India. He is a Co-Principal Investigator for the Project from Sri Lanka Technological Campus (SLTC), Srilanka. He has published several research articles in various reputed journals and international conferences. He delivered several guest lectures and keynote speech in various premier institutes. His research interests include PHY layer prospective of 5G and beyond wireless communication and signal processing.

**DUSHANTHA NALIN K. JAYAKODY** (Senior Member, IEEE) received the M.Sc. degree in electronics and communications engineering from the Department of Electrical and Electronics Engineering, Eastern Mediterranean University, Türkiye, under the university full graduate scholarship, and the Ph.D. degree in electronics and communications engineering from University College Dublin, Ireland, in 2014. From 2014 to 2016, he was a Postdoctoral Research Fellow with the University of Tartu, Estonia, and the University of Bergen, Norway. He held a visiting and/or sabbatical positions with the Center for Telecommunications Research, The University of Sydney, Australia, in 2015, and Texas A&M University, in 2018. From 2016 to 2021, he was a Professor with the School of Computer Science and Robotics, National Research Tomsk Polytechnic University (TPU), Russia. He was a Visiting Professor with the University of Jyvaskyla, Finland, in 2019 and 2022, within the framework of the Academy of Finland. He was a Visiting Professor with the University of Juiz de Fora, Brazil, in 2019. From 2019 to 2022, he was a Resource Person/Visiting Professor with the Department of Electronics and Communication Engineering, National Institute of Tiruchirappalli, India, within the SPARC Project of the Ministry of Human Resources, India. He is currently the Director of Postgraduate and Research with Sri Lanka Technological Campus (SLTC), Padukka, Sri Lanka, and has been the Founding Head of the Centre of Telecommunication Research, SLTC, since January 2019. In his career, so far, he has attracted nearly 6M USD research funding from many international grant agencies, such as European Commission, Russian Science Foundation, and Ministry of Human Resource India. He has published nearly 200 international peer-reviewed journals, conference papers, and books. His research interests include PHY and NET layer prospective of 5G communications technologies, such as NOMA for 5G, cooperative wireless communications, device to device communications, LDPC codes, and autonomous aerial vehicles. He is a fellow of IET. He also serves as an Area Editor for the *Physical Communications* (Elsevier), *Information* journal (MDPI), *Sensors* (MDPI), and *Internet Technology Letters* (Wiley). Also, he serves on the Advisory Board for *Multidisciplinary Science Journal* (MDPI). In addition, he serves as a reviewer for various IEEE TRANSACTIONS and other journals.